Letter to the Editor

Underestimation of liver hemangioma perfusion fraction by standard intravoxel incoherent motion diffusion magnetic resonance imaging

Yì Xiáng J. Wáng[1]^, Akmal Sabarudin[2]

[1]Department of Imaging and Interventional Radiology, Faculty of Medicine, The Chinese University of Hong Kong, Hong Kong SAR, China; [2]Diagnostic Imaging and Radiotherapy Program, Faculty of Health Sciences, The National University of Malaysia, Kuala Lumpur, Malaysia

Correspondence to: Yì Xiáng J. Wáng, MMed, PhD. Department of Imaging and Interventional Radiology, Faculty of Medicine, The Chinese University of Hong Kong, 30-32 Ngan Shing Street, Shatin, New Territories, Hong Kong SAR, China. Email: yixiang_wang@cuhk.edu.hk.

Submitted Nov 21, 2023. Accepted for publication Dec 20, 2023. Published online Jan 12, 2024.
doi: 10.21037/qims-23-1651
View this article at: https://dx.doi.org/10.21037/qims-23-1651

Liver hemangioma is one of the most common benign liver lesions. It is frequently diagnosed as an incidental finding on imaging, as most patients are asymptomatic. Hemangiomas are thought to be congenital in origin, non-neoplastic. Histologically, hemangioma is a mesenchymal lesion consisting of blood-filled vascular cavities of different sizes, surrounded by a simple layer of flat endothelial cells, supported by fibrous connective tissue. The cavernous hemangioma is the most common histological subtype and corresponds to the classic description of the hemangioma in imaging. Cavernous hemangioma consists of large vascular spaces with a central cavernous zone, and not very extensive connective tissue. Capillary hemangioma presents smaller vascular spaces and more extensive connective tissue. Capillary hemangioma is also known as fast-flow hemangioma and accounts for 16% of all hemangiomas. Due to its being a vascular lesion, liver hemangioma has been typically shown to be associated with very high blood volume and blood flow (1-9). Dynamic computed tomography (CT) studies consistently demonstrate liver hemangioma has much higher values of blood volume and blood flow compared with liver tissue or liver solid tumors (*Table 1*) (1-7).

On magnetic resonance imaging (MRI), liver hemangioma presents very high intensity signal on T2-weighted images, a low intensity signal on T1-weighted images and a high value of the apparent diffusion coefficient (ADC) (10). The mean T2 relaxation time of liver hemangioma has been reported to be 100 ms (0.35 T) (11), 153.9 ms (3.0 T) (12), 166.5 ms (13), or 178 ms (1.5 T) (14). The mean ADC of liver hemangioma has been reported to be 1.69×10^{-3} mm^2/s (1.5 T, b=50, 600 s/mm^2) (15), 1.87×10^{-3} mm^2/s (3.0 T, b=0, 500 s/mm^2) (16), 1.94×10^{-3} mm^2/s (3.0 T, b=0, 800 s/mm^2) (17), and 2.04×10^{-3} mm^2/s (3.0 T, b=0, 500 s/mm^2) (18). Recently, Wáng *et al.* (19-21) proposed that *in vivo* ADC measure is strongly associated with T2 relaxation time. Wáng *et al.* (20) divided T2 time into short T2 time band (<60 ms), intermediate T2 time band (60–80 ms), and long T2 time band (>80 ms, all 3 T values). For the short T2 time band, there is a negative correlation between T2 time and ADC. For the long T2 time band, there is a positive correlation between T2 time and ADC. Considering that a number of studies have shown that liver cyst has a longer T2 than liver hemangioma (12,22) and thus liver hemangioma will have a shorter T2 than the gallbladder, the position of liver hemangioma on the T2-ADC curve is shown in *Figure 1*. It appears that the measured ADC for hemangioma is higher than the ADC predicted from T2 if hemangioma were a solid/cellular tumor. This reflects the liquid nature of the hemangioma. In a gadolinium-enhanced dynamic MRI study, Nam *et al.* (23) reported that ADC values were

^ ORCID: 0000-0001-5697-0717.

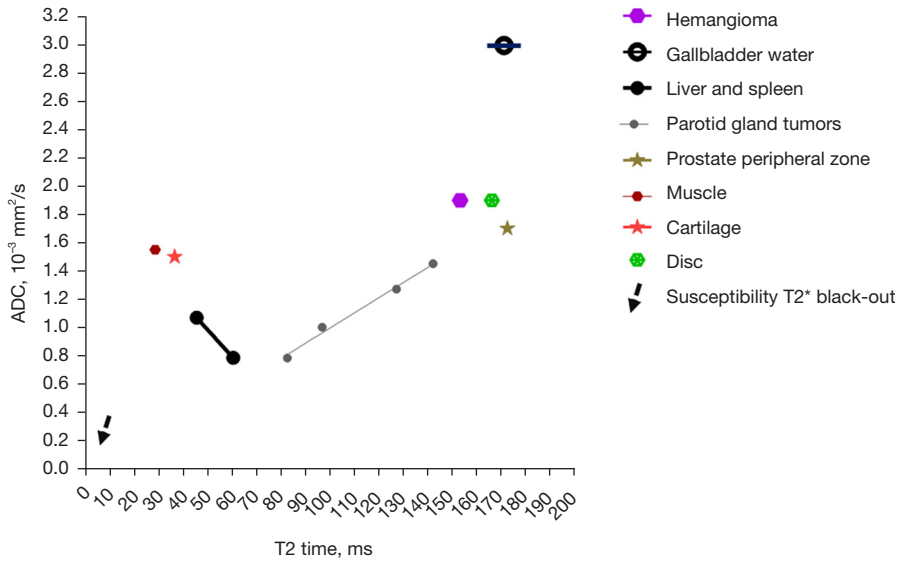

Figure 1 Relationship between T2 and ADC at 3 T. The graph is initially from Wáng *et al.* (20,21). Data sources for spleen, parotid gland tumors, and prostate see Wáng and Ma (20). Data sources for muscle, cartilage, liver, and intervertebral disc see Wáng *et al.* (21). Hemangioma is assumed to have a T2 of 153 ms and an ADC of 1.9×10^{-3} mm^2/s. Dotted arrow denotes susceptibility T2* black-out, which is observed with structures having a very short intrinsic T2 signal due to very short T2*. In this graph, dotted arrow is for illustration only, and does not reflect true quantitative values for susceptibility T2* black-out. ADC, apparent diffusion coefficient.

Table 1 A comparison of blood volume and blood flow of liver hemangioma compared with liver tissue and liver solid tumors

Authors	Parameters measured
Boas *et al.* (1)	Perfusion CT HAC (mL/mL %): cirrhotic liver, −13±7; HCC, 10±11; hemangioma: 64±23
Boas *et al.* (1)	Perfusion CT PVC (mL/mL %): cirrhotic liver, 31±14; HCC, 23±17; hemangioma: 33±29
Gadupudi *et al.* (2)	Perfusion CT blood volume (mL/100 g): liver, 13.1; hemangioma, 26.8
Gadupudi *et al.* (2)	Perfusion CT blood flow (mL/100 g/min): liver, 215.7; hemangioma, 765.9
Gadupudi *et al.* (2)	Perfusion CT blood volume (mL/100 g): liver, 15.1; HCC: 19.3
Gadupudi *et al.* (2)	Perfusion CT blood flow (mL/100 g/min): liver, 132.2; HCC, 462.2
Singh *et al.* (3)	Perfusion CT blood volume (mL/100 g): liver, 26.9±9.5; HCC, 34.5±12.2; hemangioma, 42.9±16.8
Singh *et al.* (3)	Perfusion CT blood flow (mL/100 g/min): liver, 168.4±44.9; HCC, 345.9±69.5; hemangioma, 554.6±211
Li *et al.* (4)	CT total perfusion volume (mL/100 mL/min): liver, 79.1±34.7; hemangioma, 132.7±132.7
Guo and Yu (5)	CT blood flow: liver, 39.8±18.7; hemangioma, 106.2±19.3
Zhang *et al.* (6)	PET blood-pool imaging (SUV): liver, 3.69±0.53; hemangioma, 6.83±1.38

Boas *et al.* (1) used the concept of HAC and PVC. HAC indicates similarity of a lesion's enhancement curve to the aortic enhancement curve, and PVC indicates similarity of a lesion's enhancement curve to the portal venous enhancement curve. An enhancement curve that has the same shape as the aortic enhancement curve, but only half the amount of enhancement, is considered to have 50% HAC. The HAC and PVC are equal to hepatic artery and portal vein blood volumes, in a simple perfusion model that assumes rapid blood flow and no vascular permeability to contrast. Blood volumes or coefficients are expressed in units of blood volume in a voxel (mL) divided by total volume of the voxel (mL) or as a percentage. Zhang *et al.* (6) used an albumin-binding PET radiotracer blood pool agent to measure SUV of hemangioma. Higher SUV is associated with larger perfusion volume. CT, computed tomography; HAC, hepatic artery coefficient; HCC, hepatocellular carcinoma; PVC, portal vein blood supply coefficient; PET, positron emission tomography; SUV, standardized uptake value.

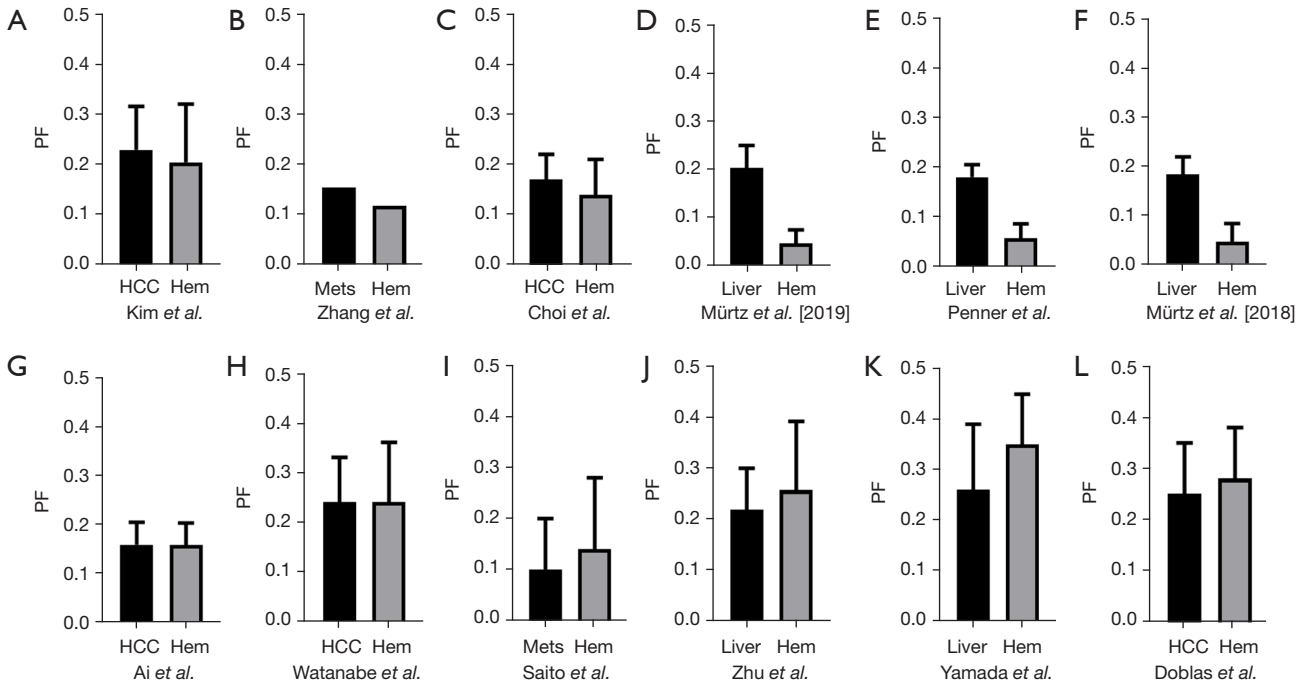

Figure 2 Literature results of IVIM measured PF of Hem, relative to liver tissue, HCC or liver Mets. Results are expressed as mean ± standard deviation, except that the median result of Zhang *et al*. is expressed. For the data of (A-F), liver, HCC or metastatic tumor PF is higher than hemangioma PF, whereas for the data of (I-L), PF of liver, HCC or metastatic tumors is lower than hemangioma PF. Data (G,H) reported similar PF for HCC and hemangioma. Data are from Kim *et al.* (17), Watanabe *et al.* (24), Choi *et al.* (25), Ai *et al.* (26), Penner *et al.* (27), Mürtz *et al.* [2019]. (28), Mürtz *et al.* [2018] (29), Zhang *et al.* (30), Saito *et al.* (31), Zhu *et al.* (32), Yamada *et al.* (33), and Doblas *et al.* (34). Data of Zhang *et al*. were approximated from the graphs in the reference. Penner *et al.* and Mürtz *et al.* used an abbreviated IVIM protocol with three *b*-values. PF, perfusion fraction; HCC, hepatocellular carcinoma; Hem, hemangioma; Mets, metastatic tumors; IVIM, intravoxel incoherent motion.

higher in the rapidly contrast enhancing hemangiomas than in the intermediately or the slowly contrast enhancing hemangiomas. Higher ADCs of rapidly enhancing hemangiomas will be related to richer intralesional vascular perfusion.

Intravoxel incoherent motion (IVIM) theory in MRI was proposed to account for the effect of vessel/capillary perfusion on the aggregate diffusion weighted magnetic resonance signal. The fast component of diffusion is related to micro-perfusion, whereas the slow component is linked to molecular diffusion. The standard IVIM modeling is based on Eq. [1]:

$$SI_{(b)}/SI_{(0)} = (1-PF)\times\exp(-b\times D_{slow}) + PF\times\exp(-b\times D_{fast}) \quad [1]$$

where $SI_{(b)}$ and $SI_{(0)}$ denote the signal intensity of images acquired with the *b*-factor value of *b* and *b*=0 s/mm^2, respectively. Three parameters can be computed. D_{slow} (or *D*) is the diffusion coefficient representing the slow molecular diffusion (unaffected by perfusion). The perfusion fraction (PF, or *f*) represents the fraction of the compartment related to (micro)circulation, which can be understood as the proportional 'incoherently flowing fluid' (i.e., blood) volume. D_{fast} (or *D**) is the perfusion-related diffusion coefficient representing speed. IVIM has been applied to evaluate the perfusion component of liver hemangioma, and the literature results of the liver hemangioma IVIM perfusion compartment are shown in *Figures 2,3* (17,24-34). The data in *Figures 2,3* are based on a PubMed systematic literature search for all English research articles which reports IVIM results of liver hemangioma, as well as liver tissue or a liver solid tumor [hepatocellular carcinoma (HCC) or liver metastasis] for comparison.

While IVIM data fitting can be unstable and the outcomes depend on many factors such as image quality, *b*-value number and distribution, the fitting method, the threshold *b*-value, etc. (35), 6 out of 12 studies showed lower hemangioma PF than its comparator (being PF of liver tissue or a solid liver tumor), two studies reported

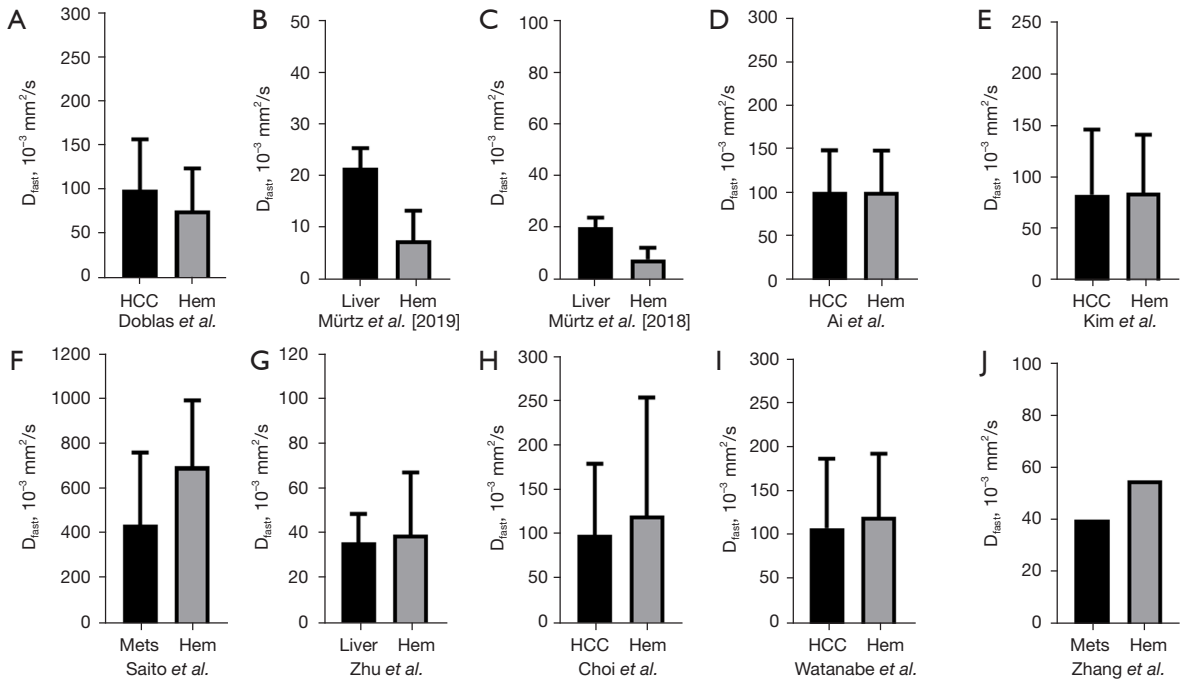

Figure 3 Literature results of IVIM measured D_{fast} of Hem, relative to liver tissue, HCC or liver Mets. Results are expressed as mean ± standard deviation, except that the median result of Zhang *et al.* is expressed. For the data of (A-C), liver or HCC D_{fast} is higher than hemangioma D_{fast}, whereas for the data of (F-J), D_{fast} of liver, HCC or metastatic tumor is lower than hemangioma D_{fast}. Data (D,E) report similar D_{fast} for HCC and hemangioma. Data are from Kim *et al.* (17), Watanabe *et al.* (24), Choi *et al.* (25), Ai *et al.* (26), Mürtz *et al.* [2019] (28), Mürtz *et al.* [2018] (29), Zhang *et al.* (30), Saito *et al.* (31), Zhu *et al.* (32), and Doblas *et al.* (34). Data of Zhang *et al.* were approximated from the graphs in the reference. Penner *et al.* and Mürtz *et al.* used an abbreviated IVIM protocol with three *b*-values.

very similar PF for hemangioma and HCC, while 4 out of 12 studies showed higher hemangioma PF than its comparator's PF. Notably, with the four studies which showed higher hemangioma PF, the magnitudes of difference were smaller than what we would expect from *Table 1*. This means, if we estimate PF based on the results from other imaging studies such as CT perfusion, then we would expect hemangioma PF in *Figure 2* will be higher to a much greater degree than the PF of liver or a solid tumor. For the results of Saito *et al.* (31), note that while HCCs are mostly hypervascular to the liver tissue, depending on their origin liver metastatic tumors can be both hypervascular or hypovascular relative to the background liver tissue (36,37).

Literature analysis in *Figure 3* shows that 3 out of 10 studies showed lower hemangioma D_{fast} than its comparator's PF, while 5 out of 10 studies showed higher hemangioma D_{fast}. Two studies reported very similar D_{fast} for hemangioma and HCC. The data fitting of D_{fast} is known to be much more unstable than that of PF (35,38). To our knowledge, blood flow speed in the hemangioma has not been measured with a physiological method. Note that perfusion CT blood flow, referring to the volume flow rate of blood through the vasculature (expressed as mL/100 g/min), is not a pure flow speed parameter. Perfusion CT mean transit time (MTT), which is the average time for blood to traverse between the arterial inflow and the venous outflow (measured in seconds), has been measured shorter for HCC relative to background liver parenchyma (39,40). Singh *et al.* (3) reported comparable MTTs for the periphery of HCC and for the periphery of hemangioma. However, conceptually MTT may also be affected by travel distance, and flow speed may be slower in the central part of a hemangioma. Though radioisotope imaging has consistently measured a high blood volume for hemangioma, the filling speed of radioisotope agents in the hemangioma is often delayed (7-9). The microbubble ultrasound blood pool agent (SonoVue) results of Haendl *et al.* (41) might have suggested that liver hemangioma has a longer MTT than that of liver metastatic tumors. Schwarz

et al. (42) used SonoVue to measure signal rising time and reported the value of 9.3±3.8 seconds for malignant tumors and 23.4±16.2 seconds for hemangioma. Rising time will be related to the flow speed and the contrast agent distribution volume. How IVIM derived D_{fast} correlate to blood flow speed in the physiological sense remains unknown.

HCC is visually associated with 'early wash-in and quick wash out' on standard tri-phase contrast-enhanced CT, and perfusion CT studies show much shorter MTT for HCC [Singh *et al.* (3): 6.8±2.8 seconds for HCC periphery and 11.4±4.2 seconds for background liver; Sahani *et al.* (39): 8.1±3.1 seconds for HCC and 14.9±2.3 for background liver]. This is partially related to that HCC receives most of its blood supply from branches of the hepatic artery. Therefore, HCC should be commonly associated with a much higher D_{fast} relative to adjacent liver tissue. However, literature reported mixed HCC IVIM D_{fast} results. Mürtz *et al.* (28), Mürtz *et al.* (29), Woo *et al.* (43), Hectors *et al.* (44) and Shan *et al.* (45) reported lower HCC D_{fast} relative to adjacent liver tissue. Zhu *et al.* (32) and Kakite *et al.* (46) reported higher HCC D_{fast} relative to adjacent liver tissue.

It has been noted that PF for HCC is also underestimated with standard IVIM imaging, and we described that the underestimation of measured PF for HCC is at least partially caused by the elongation of T2 of HCC relative to the liver (47). The same will apply to the case of hemangioma, the much higher T2 of hemangioma (say, 154 ms) relative to the liver (say, 42 ms) can contribute to the underestimation of measured hemangioma PF by standard IVIM imaging. The analysis in this letter further adds to the uncertainties on how IVIM measure results can correlate to other physiological measures (35,48-50).

In real practice, there are a small percentage of "variants" and "atypias" of hemangioma (51). For example, in rare cases, hemangioma may degenerate with extensive fibrosis, and these are called thrombosed or hyalinised hemangioma or sclerosed hemangioma (52). The discussion in the letter mainly concerns typical hemangiomas.

Acknowledgments

Funding: This work was supported by the Hong Kong GRF Project (No. 14112521).

Footnote

Conflicts of Interest: Both authors have completed the ICMJE uniform disclosure form (available at https://qims.amegroups.com/article/view/10.21037/qims-23-1651/coif). Y.X.J.W. serves as the Editor-in-Chief of *Quantitative Imaging in Medicine and Surgery*. The other author has no conflicts of interest to declare.

Ethical Statement: The authors are accountable for all aspects of the work in ensuring that questions related to the accuracy or integrity of any part of the work are appropriately investigated and resolved.

References

1. Boas FE, Kamaya A, Do B, Desser TS, Beaulieu CF, Vasanawala SS, Hwang GL, Sze DY. Classification of hypervascular liver lesions based on hepatic artery and portal vein blood supply coefficients calculated from triphasic CT scans. J Digit Imaging 2015;28:213-23.
2. Gadupudi V, Ramachandran R, Pulivadula Mohanarangam VS. The Role of Computed Tomography Perfusion in Various Focal Liver Lesions. Cureus 2022;14:e32420.
3. Singh J, Sharma S, Aggarwal N, Sood RG, Sood S, Sidhu R. Role of Perfusion CT Differentiating Hemangiomas from Malignant Hepatic Lesions. J Clin Imaging Sci 2014;4:10.
4. Li M, Chen Y, Gao Z, Zhu K, Yin X. Evaluation of the blood flow in common hepatic tumors by multi-slice spiral CT whole-liver perfusion imaging. Zhonghua Zhong Liu Za Zhi 2015;37:904-8.
5. Guo M, Yu Y. Application of 128 slice 4D CT whole liver perfusion imaging in hepatic tumor. Cell Biochem Biophys 2014;70:173-8.
6. Zhang J, Lang L, Zhu Z, Li F, Niu G, Chen X. Clinical Translation of an Albumin-Binding PET Radiotracer 68Ga-NEB. J Nucl Med 2015;56:1609-14.
7. Green L, Konwiser M, Ryo UY, Bekerman C, Pinsky SM. Is routine hepatic flow study cost effective? A case of hepatic cavernous hemangioma evaluated with dynamic flow study and delayed blood pool images. J Natl Med Assoc 1984;76:78-80.

8. Rossleigh MA, Singer I, Bautovich GJ, McLaughlin AF, Uren RF, Dyer IA, Morris JG. Blood-pool studies of the liver. Diagnostic patterns exist in cavernous haemangioma. Med J Aust 1984;140:337-40.
9. Birnbaum BA, Weinreb JC, Megibow AJ, Sanger JJ, Lubat E, Kanamuller H, Noz ME, Bosniak MA. Definitive diagnosis of hepatic hemangiomas: MR imaging versus Tc-99m-labeled red blood cell SPECT. Radiology 1990;176:95-101.
10. Duran R, Ronot M, Kerbaol A, Van Beers B, Vilgrain V. Hepatic hemangiomas: factors associated with T2 shine-through effect on diffusion-weighted MR sequences. Eur J Radiol 2014;83:468-78.
11. Ohtomo K, Itai Y, Furui S, Yashiro N, Yoshikawa K, Iio M. Hepatic tumors: differentiation by transverse relaxation time (T2) of magnetic resonance imaging. Radiology 1985;155:421-3.
12. Szklaruk J, Son JB, Starr BF, Sun J, Davila A, Bhosale PR, Ma J. Evaluation of feasibility and image quality of a new radial quantitative T2 weighted imaging sequence for liver MRI. Clin Imaging 2020;66:77-81.
13. Cittadini G, Santacroce E, Giasotto V, Rescinito G. Focal liver lesions: characterization with quantitative analysis of T2 relaxation time in TSE sequence with double echo time. Radiol Med 2004;107:166-73.
14. Goldberg MA, Hahn PF, Saini S, Cohen MS, Reimer P, Brady TJ, Mueller PR. Value of T1 and T2 relaxation times from echoplanar MR imaging in the characterization of focal hepatic lesions. AJR Am J Roentgenol 1993;160:1011-7.
15. Holzapfel K, Bruegel M, Eiber M, Ganter C, Schuster T, Heinrich P, Rummeny EJ, Gaa J. Characterization of small (≤10 mm) focal liver lesions: value of respiratory-triggered echo-planar diffusion-weighted MR imaging. Eur J Radiol 2010;76:89-95.
16. Goshima S, Kanematsu M, Kondo H, Yokoyama R, Kajita K, Tsuge Y, Shiratori Y, Onozuka M, Moriyama N. Hepatic hemangioma: correlation of enhancement types with diffusion-weighted MR findings and apparent diffusion coefficients. Eur J Radiol 2009;70:325-30.
17. Kim HC, Seo N, Chung YE, Park MS, Choi JY, Kim MJ. Characterization of focal liver lesions using the stretched exponential model: comparison with monoexponential and biexponential diffusion-weighted magnetic resonance imaging. Eur Radiol 2019;29:5111-20.
18. Parikh T, Drew SJ, Lee VS, Wong S, Hecht EM, Babb JS, Taouli B. Focal liver lesion detection and characterization with diffusion-weighted MR imaging: comparison with standard breath-hold T2-weighted imaging. Radiology 2008;246:812-22.
19. Wáng YXJ, Zhao KX, Ma FZ, Xiao BH. The contribution of T2 relaxation time to MRI-derived apparent diffusion coefficient (ADC) quantification and its potential clinical implications. Quant Imaging Med Surg 2023;13:7410-6.
20. Wáng YXJ, Ma FZ. A tri-phasic relationship between T2 relaxation time and magnetic resonance imaging (MRI)-derived apparent diffusion coefficient (ADC). Quant Imaging Med Surg 2023;13:8873-80.
21. Wáng YXJ, Aparisi Gómez MP, Ruiz Santiago F, Bazzocchi A. The relevance of T2 relaxation time in interpreting MRI apparent diffusion coefficient (ADC) map for musculoskeletal structures. Quant Imaging Med Surg 2023;13:7657-66.
22. Farraher SW, Jara H, Chang KJ, Ozonoff A, Soto JA. Differentiation of hepatocellular carcinoma and hepatic metastasis from cysts and hemangiomas with calculated T2 relaxation times and the T1/T2 relaxation times ratio. J Magn Reson Imaging 2006;24:1333-41.
23. Nam SJ, Park KY, Yu JS, Chung JJ, Kim JH, Kim KW. Hepatic cavernous hemangiomas: relationship between speed of intratumoral enhancement during dynamic MRI and apparent diffusion coefficient on diffusion-weighted imaging. Korean J Radiol 2012;13:728-35.
24. Watanabe H, Kanematsu M, Goshima S, Kajita K, Kawada H, Noda Y, Tatahashi Y, Kawai N, Kondo H, Moriyama N. Characterizing focal hepatic lesions by free-breathing intravoxel incoherent motion MRI at 3.0 T. Acta Radiol 2014;55:1166-73.
25. Choi IY, Lee SS, Sung YS, Cheong H, Lee H, Byun JH, Kim SY, Lee SJ, Shin YM, Lee MG. Intravoxel incoherent motion diffusion-weighted imaging for characterizing focal hepatic lesions: Correlation with lesion enhancement. J Magn Reson Imaging 2017;45:1589-98.
26. Ai Z, Han Q, Huang Z, Wu J, Xiang Z. The value of multiparametric histogram features based on intravoxel incoherent motion diffusion-weighted imaging (IVIM-DWI) for the differential diagnosis of liver lesions. Ann Transl Med 2020;8:1128.
27. Penner AH, Sprinkart AM, Kukuk GM, Gütgemann I, Gieseke J, Schild HH, Willinek WA, Mürtz P. Intravoxel incoherent motion model-based liver lesion characterisation from three b-value diffusion-weighted MRI. Eur Radiol 2013;23:2773-83.
28. Mürtz P, Pieper CC, Reick M, Sprinkart AM, Schild HH, Willinek WA, Kukuk GM. Is liver lesion characterisation by simplified IVIM DWI also feasible at 3.0 T? Eur Radiol

2019;29:5889-900.
29. Mürtz P, Sprinkart AM, Reick M, Pieper CC, Schievelkamp AH, König R, Schild HH, Willinek WA, Kukuk GM. Accurate IVIM model-based liver lesion characterisation can be achieved with only three b-value DWI. Eur Radiol 2018;28:4418-28.
30. Zhang HX, Zhang XS, Kuai ZX, Zhou Y, Sun YF, Ba ZC, He KB, Sang XQ, Yao YF, Chu CY, Zhu YM. Determination of Hepatocellular Carcinoma and Characterization of Hepatic Focal Lesions with Adaptive Multi-Exponential Intravoxel Incoherent Motion Model. Transl Oncol 2018;11:1370-8.
31. Saito K, Yoshimura N, Shirota N, Saguchi T, Sugimoto K, Tokuuye K. Distinguishing liver haemangiomas from metastatic tumours using gadolinium ethoxybenzyl diethylenetriamine pentaacetic acid-enhanced diffusion-weighted imaging at 1.5T MRI. J Med Imaging Radiat Oncol 2016;60:599-606.
32. Zhu L, Cheng Q, Luo W, Bao L, Guo G. A comparative study of apparent diffusion coefficient and intravoxel incoherent motion-derived parameters for the characterization of common solid hepatic tumors. Acta Radiol 2015;56:1411-8.
33. Yamada I, Aung W, Himeno Y, Nakagawa T, Shibuya H. Diffusion coefficients in abdominal organs and hepatic lesions: evaluation with intravoxel incoherent motion echo-planar MR imaging. Radiology 1999;210:617-23.
34. Doblas S, Wagner M, Leitao HS, Daire JL, Sinkus R, Vilgrain V, Van Beers BE. Determination of malignancy and characterization of hepatic tumor type with diffusion-weighted magnetic resonance imaging: comparison of apparent diffusion coefficient and intravoxel incoherent motion-derived measurements. Invest Radiol 2013;48:722-8.
35. Wang YXJ, Huang H, Zheng CJ, Xiao BH, Chevallier O, Wang W. Diffusion-weighted MRI of the liver: challenges and some solutions for the quantification of apparent diffusion coefficient and intravoxel incoherent motion. Am J Nucl Med Mol Imaging 2021;11:107-42.
36. Schmid-Tannwald C, Thomas S, Ivancevic MK, Dahi F, Rist C, Sethi I, Oto A. Diffusion-weighted MRI of metastatic liver lesions: is there a difference between hypervascular and hypovascular metastases? Acta Radiol 2014;55:515-23.
37. Abdullah SS, Pialat JB, Wiart M, Duboeuf F, Mabrut JY, Bancel B, Rode A, Ducerf C, Baulieux J, Berthezene Y. Characterization of hepatocellular carcinoma and colorectal liver metastasis by means of perfusion MRI. J Magn Reson Imaging 2008;28:390-5.
38. Zheng CJ, Xiao BH, Huang H, Zhou N, Yan TY, Wáng YXJ. Bi-exponential fitting excluding b=0 data improves the scan-rescan stability of liver IVIM parameter measures and particularly so for the perfusion fraction. Quant Imaging Med Surg 2022;12:3288-99.
39. Sahani DV, Holalkere NS, Mueller PR, Zhu AX. Advanced hepatocellular carcinoma: CT perfusion of liver and tumor tissue--initial experience. Radiology 2007;243:736-43.
40. Zhu AX, Holalkere NS, Muzikansky A, Horgan K, Sahani DV. Early antiangiogenic activity of bevacizumab evaluated by computed tomography perfusion scan in patients with advanced hepatocellular carcinoma. Oncologist 2008;13:120-5.
41. Haendl T, Strobel D, Steinebrunner N, Frieser M, Hahn EG, Bernatik T. Hepatic transit time in benign liver lesions. Ultraschall Med 2008;29:184-9.
42. Schwarz S, Clevert DA, Ingrisch M, Geyer T, Schwarze V, Rübenthaler J, Armbruster M. Quantitative Analysis of the Time-Intensity Curve of Contrast-Enhanced Ultrasound of the Liver: Differentiation of Benign and Malignant Liver Lesions. Diagnostics (Basel) 2021;11:1244.
43. Woo S, Lee JM, Yoon JH, Joo I, Han JK, Choi BI. Intravoxel incoherent motion diffusion-weighted MR imaging of hepatocellular carcinoma: correlation with enhancement degree and histologic grade. Radiology 2014;270:758-67.
44. Hectors SJ, Wagner M, Besa C, Bane O, Dyvorne HA, Fiel MI, Zhu H, Donovan M, Taouli B. Intravoxel incoherent motion diffusion-weighted imaging of hepatocellular carcinoma: Is there a correlation with flow and perfusion metrics obtained with dynamic contrast-enhanced MRI? J Magn Reson Imaging 2016;44:856-64.
45. Shan Y, Zeng MS, Liu K, Miao XY, Lin J, Fu Cx, Xu PJ. Comparison of Free-Breathing With Navigator-Triggered Technique in Diffusion Weighted Imaging for Evaluation of Small Hepatocellular Carcinoma: Effect on Image Quality and Intravoxel Incoherent Motion Parameters. J Comput Assist Tomogr 2015;39:709-15.
46. Kakite S, Dyvorne HA, Lee KM, Jajamovich GH, Knight-Greenfield A, Taouli B. Hepatocellular carcinoma: IVIM diffusion quantification for prediction of tumor necrosis compared to enhancement ratios. Eur J Radiol Open 2016;3:1-7.
47. Ma FZ, Wáng YXJ. T2 relaxation time elongation of hepatocellular carcinoma relative to native liver tissue leads to an underestimation of perfusion fraction measured by standard intravoxel incoherent motion magnetic resonance

imaging. Quant Imaging Med Surg 2023. doi: 10.21037/qims-23-1437
48. Wáng YXJ. Observed paradoxical perfusion fraction elevation in steatotic liver: An example of intravoxel incoherent motion modeling of the perfusion component constrained by the diffusion component. NMR Biomed 2021;34:e4488.
49. Wáng YXJ. Mutual constraining of slow component and fast component measures: some observations in liver IVIM imaging. Quant Imaging Med Surg 2021;11:2879-87.
50. Wáng YXJ. A reduction of perfusion can lead to an artificial elevation of slow diffusion measure: examples in acute brain ischemia MRI intravoxel incoherent motion studies. Ann Transl Med 2021;9:895.
51. Caseiro-Alves F, Brito J, Araujo AE, Belo-Soares P, Rodrigues H, Cipriano A, Sousa D, Mathieu D. Liver haemangioma: common and uncommon findings and how to improve the differential diagnosis. Eur Radiol 2007;17:1544-54.
52. Ridge CA, Shia J, Gerst SR, Do RK. Sclerosed hemangioma of the liver: concordance of MRI features with histologic characteristics. J Magn Reson Imaging 2014;39:812-8.

Cite this article as: Wáng YXJ, Sabarudin A. Underestimation of liver hemangioma perfusion fraction by standard intravoxel incoherent motion diffusion magnetic resonance imaging. Quant Imaging Med Surg 2024;14(2):2128-2135. doi: 10.21037/qims-23-1651

